Available online at www.sciencedirect.com
SCIENCE DIRECT®
Journal of Organometallic Chemistry 690 (2005) 2106–2120
Journal of Organometallic Chemistry
www.elsevier.com/locate/jorganchem

Trifluoroethanol: key solvent for palladium-catalyzed polymerization reactions

Alessandro Scarel [a], Jérôme Durand [a], Davide Franchi [a], Ennio Zangrando [a], Giovanni Mestroni [a], Barbara Milani [a,*], Serafino Gladiali [b], Carla Carfagna [c], Barbara Binotti [c], Simona Bronco [d,e], Tania Gragnoli [e]

[a] *Dipartimento di Scienze Chimiche, Università di Trieste, Via Licio Giorgieri 1, 34127 Trieste, Italy*
[b] *Dipartimento di Chimica, Università di Sassari, Via Vienna 2, 07100, Sassari, Italy*
[c] *Istituto di Scienze Chimiche, Università di Urbino, Piazza, Rinascimento 6, Urbino, Italy*
[d] *PolyLab-INFM-Pisa c/o, Dipartimento di Chimica e Chimica Industriale, Università di Pisa, Via Risorgimento 35, 56126 Pisa, Italy*
[e] *Dipartimento di Chimica e Chimica Industriale, Università di Pisa c/o Waste Recycling, Via Risorgimento 35, 56126 Pisa, Italy*

Received 22 December 2004; accepted 4 January 2005
Available online 9 February 2005

Abstract

A series of cationic palladium complexes of general formula $[Pd(CH_3)(NCCH_3)(N–N)][X]$ (N–N = phen **1**, 3-*sec*-butyl-1,10-phenanthroline (3-*s*Bu-phen) **2**, bpy **3**, (−)-(*S*,*S*)-3,3′-(1,2-dimethylethylenedioxy)-2,2′-bipyridine (bbpy) **4**, (+)-(*R*)-3,3′-(1-methylethylenedioxy)-2,2′-bipyridine (pbpy) **5**, *N*,*N*′-bis(2,6-diisopropylphenyl)-2,3-butanediimine (iso-DAB) **6**; $X = PF_6^-$ **a**, OTf (OTf = triflate) **b**) containing different nitrogen-donor ligands were prepared from the corresponding neutral chloro derivatives $[Pd(CH_3)(Cl)(N–N)]$ (**1c**–**6c**). They were characterized by ^1H NMR spectroscopy and elemental analysis. Single crystals suitable for X-ray determination were obtained for complexes $[Pd(CH_3)(NCCH_3)(bbpy)][PF_6]$ (**4a**), $[Pd(CH_3)(NCCH_3)(iso\text{-}DAB)][PF_6]$ (**6a**) and $[Pd(Cl)_2(bbpy)]$ (**4c**′). The latter is the result of an exchange reaction of the methyl group, present in complex **4c**, with a chloride, that occurred after dissolution of **4c** in $CDCl_3$, for 1 week at 0 °C. The catalytic behavior of complexes **1a**–**5a** and **1b**–**5b** in the CO/styrene copolymerization was studied in CH_2Cl_2 and 2,2,2-trifluoroethanol (TFE) evidencing the positive effect of the fluorinated alcohol both in terms of productivity and molecular weight values of the polymers obtained. Influence of the nitrogen ligand, the anion and the reaction time in both solvents were investigated and is discussed in detail. Encouraging preliminary results were also obtained in the synthesis of polyethylene, in TFE, catalyzed by $[Pd(CH_3)(NCCH_3)(iso\text{-}DAB)][PF_6]$ (**6a**).

Keywords: Palladium; Nitrogen-donor ligands; Carbon monoxide; Olefins; Polyketone; Catalysis

1. Introduction

Metal promoted polymerization represents a powerful tool for the atom-economic, environmentally friendly, synthesis of new polymeric materials [1]. Through the proper choice of the components of the polymerization catalytic system it is possible to control the structure of the synthesized macromolecules and, as a consequence, to synthesize polymers for well defined applications. The discovery by Brookhart and Gibson [2] of very efficient, non-metallocene, catalysts for the polyolefins synthesis had a galvanizing effect on the researches in this field. In particular, Brookhart [3] reported that the palladium complex $[Pd(CH_3)(OEt_2)$-

* Corresponding author. Tel.: +39 040 5583955; fax: +39 040 5583903.
E-mail addresses: milani@dsch.univ.trieste.it (B. Milani).

0022-328X/$ - see front matter © 2005 Elsevier B.V. All rights reserved.
doi:10.1016/j.jorganchem.2005.01.004

(iso-DAB)][BArF] (iso-DAB = ArN=C(CH_3)–C(CH_3)=NAr (Ar = 2,6-(*i*Pr)$_2$-C_6H_3); BArF = [B(3,5-(CF_3)$_2$-Ph)$_4$]$^-$) promotes the polyethylene synthesis, in dichloromethane, at 25 °C, yielding highly branched polyethylene with a productivity of 0.25 kg PE/g Pd h (kg PE/g Pd h = kilograms of polyethylene per gram of palladium per hour).

A wide variety of palladium complexes with nitrogen-donor ligands (N–N) has been also developed for the stereocontrolled synthesis of carbon monoxide/vinyl arenes co- and terpolymers [4]. Usually, the synthesis of syndiotactic CO/aromatic olefin copolymers is promoted by monochelated complexes in methanol, whereas the corresponding polyketones with an isotactic microstructure are obtained with organometallic monochelated derivatives of general formula [Pd(CH_3)($NCCH_3$)(N*–N*)][BArF], in dichloromethane, where N*–N* are chiral, enantiomerically pure ligands of C_2 symmetry [4d–4i].

The main problem encountered with these catalytic systems is related to the stability of the active species that easily decomposes to inactive palladium metal. For the synthesis of the syndiotactic CO/vinyl arene polyketones we studied in detail the factors affecting the catalyst stability and we found that the catalyst lifetime is greatly enhanced when the copolymerization reaction is carried out in 2,2,2-trifluoroethanol (TFE) and when bischelated complexes [Pd(N–N)$_2$][PF_6]$_2$ (N–N = 1,10-phenanthroline (phen), 2,2′-bipyridine (bpy) and their symmetrically and unsymmetrically substituted derivatives) are used [5]. It is of great interest to solve the problem of catalyst stability even in the synthesis of the polyketones with an isotactic microstructure, since, thanks to their main chain chirality, they might have very useful applications.

As first step toward this goal, we decided to investigate if the positive effect of the fluorinated solvent is maintained when monochelated complexes are used in place of the corresponding bischelated derivatives. In this paper we report the synthesis and characterization of monochelated, monocationic organometallic palladium (II) complexes of general formula [Pd(CH_3)($NCCH_3$)(N–N)][X] (N–N = phen **1** [4c], 3-*sec*-butyl-1,10-phenanthroline (3-*s*Bu-phen) **2**, bpy **3**, (−)-(*S*,*S*)-3,3′-(1,2-dimethylethylenedioxy)-2,2′-bipyridine (bbpy) **4**, (+)-(*R*)-3,3′-(1-methylethylenedioxy)-2,2′-bipyridine (pbpy) **5**, *N*,*N*′-bis(2,6-diisopropylphenyl)-2,3-buthanediimine (iso-DAB) **6**; X = PF_6^- **a**, OTf (OTf = triflate) **b**) and their catalytic behavior in CO/styrene copolymerization together with some very preliminary results in polyethylene synthesis.

2. Results and discussion

2.1. Synthesis and characterization of [Pd(CH_3)($NCCH_3$)(N–N)][X] complexes, 1a–6a, 1b–5b

The palladium complexes **1a**–**6a** and **1b**–**5b** are easily synthesized starting from [Pd(CH_3COO)$_2$] and following a five-steps procedure reported in the literature [6]. The key step of this procedure is the dehalogenation reaction of the neutral derivatives [Pd(CH_3)(Cl)(N–N)] (**1c**–**6c**, Scheme 1).

Both the neutral and monocationic series of complexes have been characterized in solid state and in solution. Single crystals of the neutral derivative [Pd(Cl)$_2$(bbpy)] (**4c**′) are obtained upon addition of diethyl ether to a solution of [Pd(CH_3)(Cl)(bbpy)] (**4c**) in chloroform, after one week at 0 °C. The X-ray analysis reveals that, during the crystallization process, an exchange reaction of the methyl group bound to palladium with chloride occurred (Fig. 1). This behavior has been recently reported also for other Pd–CH_3 complexes with nitrogen-donor ligands [7].

Two crystallographically independent molecules, A and B, were detected in the unit cell of complex **4c**′. Fig. 1 shows the ORTEP drawing with pertinent labeling scheme of one molecule of **4c**′. A selection of bond lengths and angles is reported in the figure caption.

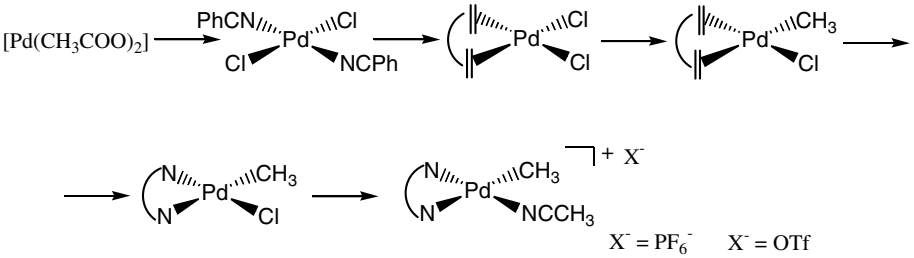

		X$^-$ = PF_6^-	X$^-$ = OTf
N-N = phen	**1c**	**1a**	**1b**
3-*s*Bu-phen	**2c**	**2a**	**2b**
bpy	**3c**	**3a**	**3b**
bbpy	**4c**	**4a**	**4b**
pbpy	**5c**	**5a**	**5b**
iso-DAB	**6c**	**6a**	

Scheme 1. Synthetic pathway of the monocationic palladium complexes **1a**–**6a**, **1b**–**5b**.

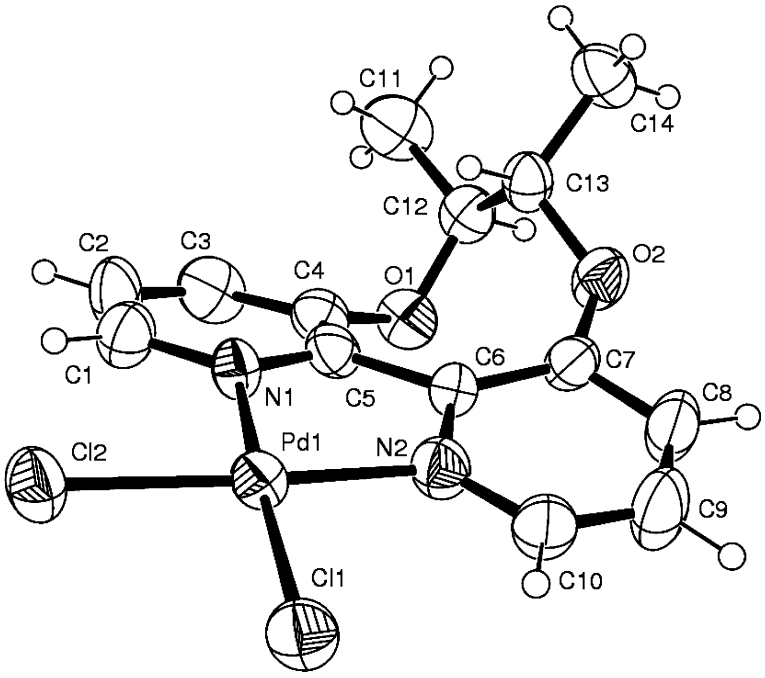

Fig. 1. ORTEP drawing (40% probability ellipsoid) of one of the two crystallographically independent neutral complexes $[Pd(Cl)_2(bbpy)]$ (**4c**′). Selected bond lengths (Å) and angles (°): Pd(1)–N(1) 2.006(8), Pd(1)–N(2) 2.025(9), Pd(1)–Cl(1) 2.299(3), Pd(1)–Cl(2) 2.297(3), N(1)–Pd(1)–N(2) 79.3(3), Cl(1)–Pd(1)–Cl(2) 88.16(10), N(1)–Pd(1)–Cl(1) 175.3(3), N(2)–Pd(1)–Cl(2) 174.6(3). Correspondent values in molecule B: 2.020(9), 2.031(9), 2.302(3), 2.305(3), 80.5(4), 89.13(12), 174.5(3), 175.4(3).

The two molecules are geometrically similar and arranged head-to-tail with each metal located over the chelating five-membered ring of the other complex (intermetallic distance of 3.655(1) Å; Fig. 2(a)). The palladium atom attains the usual square planar coordination being bound to two chlorides and chelated by the nitrogen donors. The pyridine rings are twisted with a dihedral angle between the planes of 28.3(6)° and 27.9(6)°, in A and B, respectively. All the Pd–N and Pd–Cl bond distances are closely comparable within their e.s.d.'s, varying in the range 2.006(8)–2.031(9) and 2.297(3)–2.305(3) Å, respectively.

For the corresponding monocationic complex $[Pd(CH_3)(NCCH_3)(bbpy)][PF_6]$ (**4a**) single crystals were directly obtained from the reaction mixture (Fig. 3). Also for this complex two crystallographically independent molecules were present in the unit cell. The X-ray diffraction analysis of **4a** provided structural results of low resolution. Nevertheless, the experiment confirms the geometry as deduced by NMR spectra. The coordination bond lengths in the two crystallographically independent complexes appear in the range usually found for Pd(II) complexes. The Pd–N distance *trans* to the methyl is longer by about 0.1 Å with respect to the other

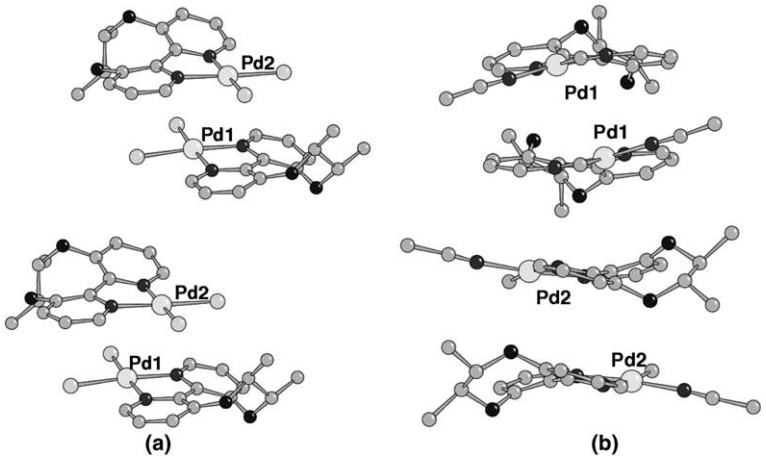

Fig. 2. Packing view of piled crystallographic independent complexes in: (a) **4c**′ (pairs of Pd1–Pd2); (b) **4a** (sequence of $-(Pd1)_2-(Pd2)_2-$).

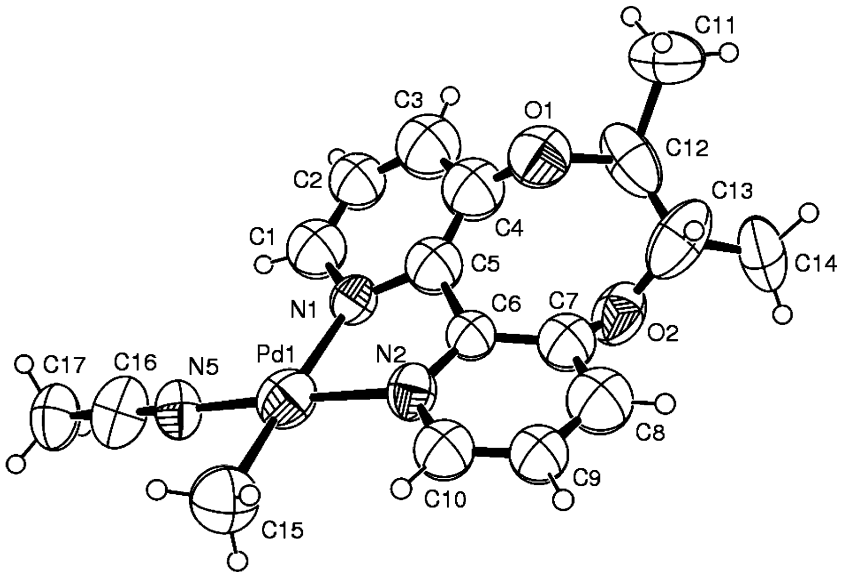

Fig. 3. ORTEP drawing (40% probability ellipsoid) of one of the two crystallographically independent complex cationic derivative $[Pd(CH_3)(NCCH_3)(bbpy)][PF_6]$ (**4a**). Selected bond lengths (Å) and angles (°) in molecule A: Pd(1)–N(1) 2.127(18), Pd(1)–N(2) 2.063(18), Pd(1)–N(5) 1.99(2), Pd(1)–C(15) 2.09(3), N(2)–Pd(1)–N(1) 79.7(7), N(5)–Pd(1)–C(15) 87.0(10), N(1)–Pd(1)–C(15) 174.5(10), N(2)–Pd(1)–N(5) 174.8(8). Correspondent values in molecule B: 2.13(2), 2.03(2), 2.01(3), 1.97(3), 77.8(9), 89.8(15), 170.4(14), 174.3(11).

atropisomeric ligand donor (2.13(2) vs. 2.04(2) Å), while the Pd–$NCCH_3$ and Pd–CH_3 bond lengths are of about 2.00(2) Å. The molecules A and B are piled along axis *c* with a sequence $–(A)_2–(B)_2–$ with an intermetallic Pd1–Pd1 distance of 3.716(3) Å between molecules A related by a twofold axis (Fig. 2(b)). This distance is close comparable to that measured in **4c′** between the two independent neutral complexes that are packed in the crystal with a sequence of type –(AB)–(AB)– along the crystallographic axis *b*. The dihedral angle between the planes containing the pyridine rings is 28.0(6)° and 27.8(6)°, in the molecule A and B, respectively.

Some geometrical parameters defining the conformation of the atropisomeric ligands in the two compounds, **4c′** and **4a**, are shown in Table 1. The atropisomeric configuration, defined by the N–C–C–N torsion angle, assumes values of opposite sign in the two compounds. Thus, the absolute configuration is *M* and *P* in **4c′** and **4a**, respectively [8,9].

As evident from Figs. 1 and 3, the two complexes exhibit a different conformation of the O–C–C–O bridge, that is described by taking into account the position of the bridge atoms with respect to the coordination plane. In **4c′** all the atoms of the O–C–C–O bridge (except for O(1)) are found on the same side out of the coordination plane. The maximum displacement is measured for one methyl group at 2.3 Å (mean value of the two molecules A and B). The eight-membered ring including the bridge assumes an overall *skew-boat* conformation. In **4a** the coordination plane bisects the C(12)–C(13) bond, leading to a conformation with the O–CH–CH_3 moieties at opposite sides (mean displacements of oxygens ±1.1 Å, methyls ±1.4 Å). These two different conformations were also found in the corresponding trifluoroacetate derivative with the pbpy ligand, $[Pd(CF_3COO)_2(pbpy)]$ [8]. In analogy with the present results, even for those complexes the *skew-boat* conformation was detected for the *M* atropisomer, while the other arrangement was observed for the *P* atropisomer.

Single crystals of $[Pd(CH_3)(NCCH_3)(iso\text{-}DAB)][PF_6]$ (**6a**) were isolated upon addition of diethyl ether to the CD_2Cl_2 solution in the NMR tube (Fig. 4). The palladium atom is surrounded by the nitrogen atoms of the chelating ligand and of acetonitrile and by the carbon atom of the methyl group. The Pd–N(1) distance is longer than the Pd–N(2) (2.143(3) vs. 2.036(3) Å, respectively) due to the relatively large *trans* influence of the methyl group. The Pd–C of 2.037(4) Å and Pd–$NCCH_3$ of 2.008(4) Å are as expected and can be compared with those found in the corresponding dimethyl and bis(acetonitrile) derivatives [10]. The coordination plane shows strictly coplanar atoms with no appreciable

Table 1
Geometrical parameters defining the conformation of bbpy ligands in the two independent complexes of **4c′** and **4a**

	4c′		**4a**	
	A	B	A	B
N(1)–C(5)–C(6)–N(2)	15.4(13)	17.5(12)	−28(3)	−22(3)
O(1)–C(12)–C(13)–O(2)	55.7(8)	55.5(9)	49(3)	50(3)
O(1)–C(12)–C(13)–C(14)	175.3(7)	173.1(9)	171(2)	168(2)
C(11)–C(12)–C(13)–O(2)	−178.1(8)	−178.7(8)	164(2)	170(3)
C(11)–C(12)–C(13)–C(14)	−58.5(10)	−61.1(12)	−74(4)	−72(4)
Py/py dihedral angle	28.3(6)	27.9(6)	28.0(6)	27.8(6)
C(4)–O(1)–C(12)	115.4(6)	114.8(6)	118(2)	120(2)
C(7)–O(2)–C(13)	123.6(6)	121.4(7)	120(2)	121(2)

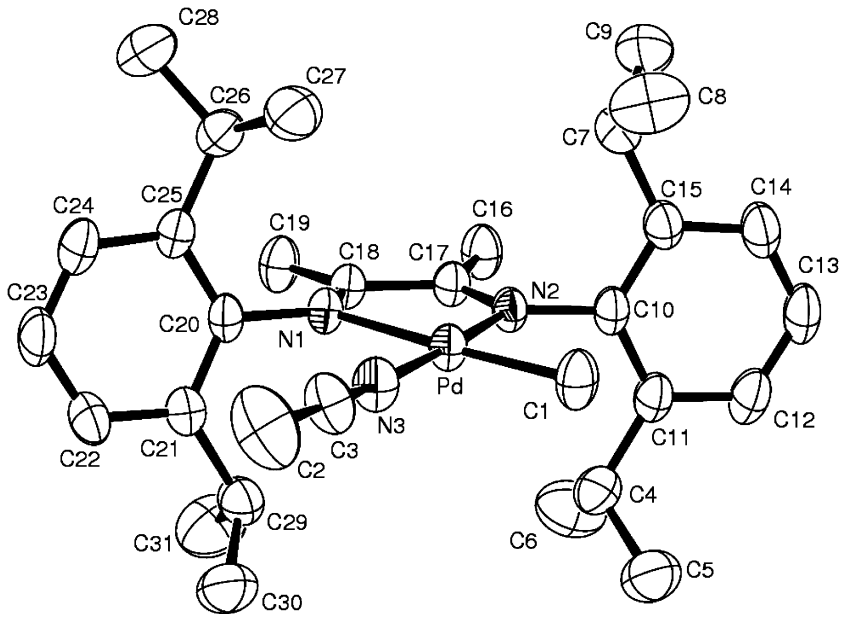

Fig. 4. ORTEP drawing (40% probability ellipsoid) of the cationic derivative $[Pd(CH_3)(NCCH_3)(iso\text{-}DAB)][PF_6]$ **6a**. Selected bond lengths (Å) and angles (°): Pd–N(1) 2.143(3), Pd–N(2) 2.036(3), Pd–N(3) 2.008(4), Pd–C(1) 2.037(4), N(1)–Pd–N(2) 77.97(11), N(1)–Pd–N(3) 98.00(13), N(1)–Pd–C(1) 173.51(15), N(2)–Pd–N(3) 175.97(13), N(2)–Pd–C(1) 95.54(16), N(3)–Pd–C(1) 88.48(17).

displacement of the metal. The two phenyl rings are arranged almost perpendicular to the butandiimino moiety (dihedral angles of 85.1(2)° and 77.9(2)°) with alkyl groups that obstruct both sides of the coordination plane. As a consequence the PF_6^- anions are far apart and do not show any interaction with the metal, as frequently observed in the solid state structures of square planar palladium compounds with this anion (Pd–F short distance of ca. 3.0 Å) [5c,11].

The characterization in solution of both neutral and cationic series of complexes was performed by ^1H NMR spectroscopy recording the spectra in $CDCl_3$ and CD_2Cl_2, respectively, at room temperature (Tables 2 and 3). For the sake of clarity we numbered the protons of phenanthrolines and bipyridines starting from the heterocyclic ring in *cis* position to the Pd–CH_3 fragment (Scheme 2) and, analogously, for the complexes with the non symmetrical ligands, the isomer with the substituent on the ligand on the same side of the Pd–CH_3 group has been conventionally called *cis* (Scheme 1).

For both series of complexes the singlet of the methyl bound to palladium falls in a range of frequency between 1.00 and 1.30 ppm; and, in the case of the cationic derivatives, the signal of acetonitrile is in the range between 2.20 and 2.65 ppm. No signal due to free CH_3CN is evident. As far as the protons of the N–N ligand are concerned, in all spectra no signal due to the free ligand is present; the number of peaks and their integration are in agreement with its coordination in a non-symmetric

Table 2
Selected ^1H NMR data for complexes $[Pd(CH_3)(Cl)(N–N)]$ (**1c**–**5c**)[a]

N–N/complex	H^2	H^9	Pd–CH_3	$\Delta\delta$[b]
phen	9.20(dd)	9.20(dd)		0
$[Pd(CH_3)(Cl)(phen)]$ (**1c**)	9.02(dd)	9.49(dd)	1.22(s)	0.47
3-*s*Bu-phen	9.04(d)	9.17(dd)		0.13
$[Pd(CH_3)(Cl)(3\text{-}sBu\text{-}phen)]$ (**2c**)	8.84(s, *cis*)	9.46(d, *cis*)	1.22(s, *cis*)	0.62
	9.31(s, *trans*)	8.99(d, *trans*)	1.21(s, *trans*)	0.32
	H^6	$H^{6\prime}$	Pd–CH_3	$\Delta\delta$[b]
bpy	8.69(dd)	8.69(dd)		0
$[Pd(CH_3)(Cl)(bpy)]$ (**3c**)	8.71(d)	9.24(d)	1.05(s)	0.53
bbpy	8.58(dd)	8.58(dd)		0
$[Pd(CH_3)(Cl)(bbpy)]$ (**4c**)	8.44(d)	8.93(d)	1.09(s)	0.49
pbpy	8.60(dd)	8.60(dd)		0
$[Pd(CH_3)(Cl)(pbpy)]$ (**5c**)	8.49(b)	9.00(t)	1.06(s)	0.51

[a] Spectra recorded in $CDCl_3$, at room temperature, δ in ppm. d, doublet; dd, double of doublets; t, triplet; s, singlet.
[b] $\Delta\delta$ is the chemical shift difference between H^2 and H^9, and between H^6 and $H^{6\prime}$.

Table 3
Selected ^{1}H NMR data for complexes [Pd(CH$_3$)(NCCH$_3$)(N–N)][X], X = PF_6^- (**1a**–**5a**), X = OTf (**1b**–**5b**)[a]

N–N, X	H^2	H^9	Pd–CH_3	$\Delta\delta$[b]
phen, PF_6 (**1a**)	8.90(dd)	9.00(dd)	1.26(s)	0.10
phen, OTf (**1b**)	8.90(dd)	9.10(dd)	1.25(s)	0.20
3-*s*Bu-phen, PF_6 (**2a**)	8.71(s, *cis*)	9.00(dd, *cis*)	1.26(s, *cis*)	0.29
	8.71(s, *trans*)	8.88(dd, *trans*)	1.28(s, *trans*)	0.27
3-*s*Bu-phen, OTf (**2b**)	8.71(s, *cis*)	9.08(d, *cis*)	1.25(s, *cis*)	0.37
	8.74(s, *trans*)	8.87(dd, *trans*)	1.27(s, *trans*)	0.23
	H^6	$H^{6\prime}$	Pd–CH_3	$\Delta\delta$[b]
bpy, PF_6 (**3a**)	8.59(d)	8.62(d)	1.10(s)	0.03
bpy, OTf (**3b**)	8.55(d)	8.70(d)	1.07(s)	0.15
bbpy, PF_6 (**4a**)	8.29(d)	8.37(d)	1.13(s)	0.08
bbpy, OTf (**4b**)	8.30(d)	8.45(d)	1.13(s)	0.15
pbpy, PF_6 (**5a**)	8.35(m)	8.35(m)	1.10(s)	0
pbpy, OTf (**5b**)	8.36(b)	8.43(b)	1.10(s)	0.07

[a] Spectra recorded in CD_2Cl_2, at room temperature, δ in ppm. d, doublet; dd, double of doublets; t, triplet; s, singlet; m, multiplet.
[b] $\Delta\delta$ is the chemical shift difference between H^2 and H^9, and between H^6 and $H^{6\prime}$.

chemical environment. In the neutral derivatives, the difference in chemical shift ($\Delta\delta$) of the signals of the "probe-protons" (protons in *ortho* to the nitrogen donors) is more pronounced than in the cationic complexes (Tables 2 and 3) due to the presence of the Pd–Cl group, which significantly shifts at high frequency the resonance of the proton in *cis* to it [6a]. The number of peaks in the spectra of complexes **2a**, **2b** and **2c**, bearing the 3-*s*Bu-phen ligand, indicates the presence in solution of *cis* and *trans* isomers (Scheme 2) in different ratio depending on the nature of the complex, being the *trans* the prevailing isomer for the neutral complex **2c** and the *cis* for the cationic derivatives **2a** and **2b** (*cis*/*trans* = 0.88 for **2c**, 1.63 for **2a**, 1.22 for **2b**).

The spectra of complexes with the atropisomeric ligands, bbpy and pbpy, are different depending on the ligand. One set of signals is present in the case of complexes **4a**, **4b** and **4c** for all the protons. The resonance of the CH protons of the butyl bridge is broad at room temperature (Fig. 5(a)), thus indicating that the rate of interconversion between the two atropisomers is comparable within the NMR timescale [12]. For complexes **5a**, **5b** and **5c** all the protons of the propyl bridge generate two sets of peaks, while only one resonance is observed for the Pd–CH_3 group and for the protons of the aromatic rings (Fig. 5(b)). Therefore, it is reasonable to assume that the two sets of signals correspond to the two atropisomers and not to the *cis* and

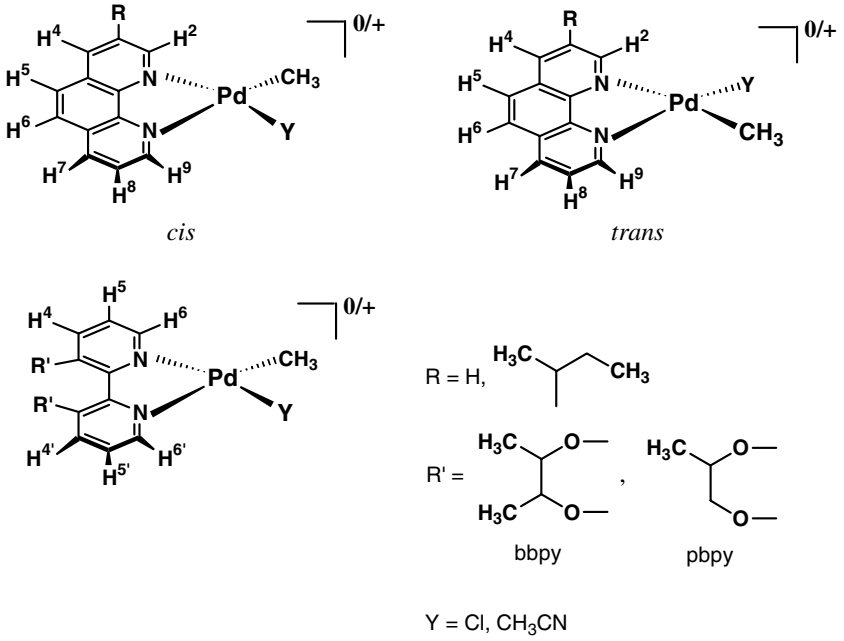

Scheme 2. Numbering scheme of ligands in the corresponding neutral and monocationic palladium complexes.

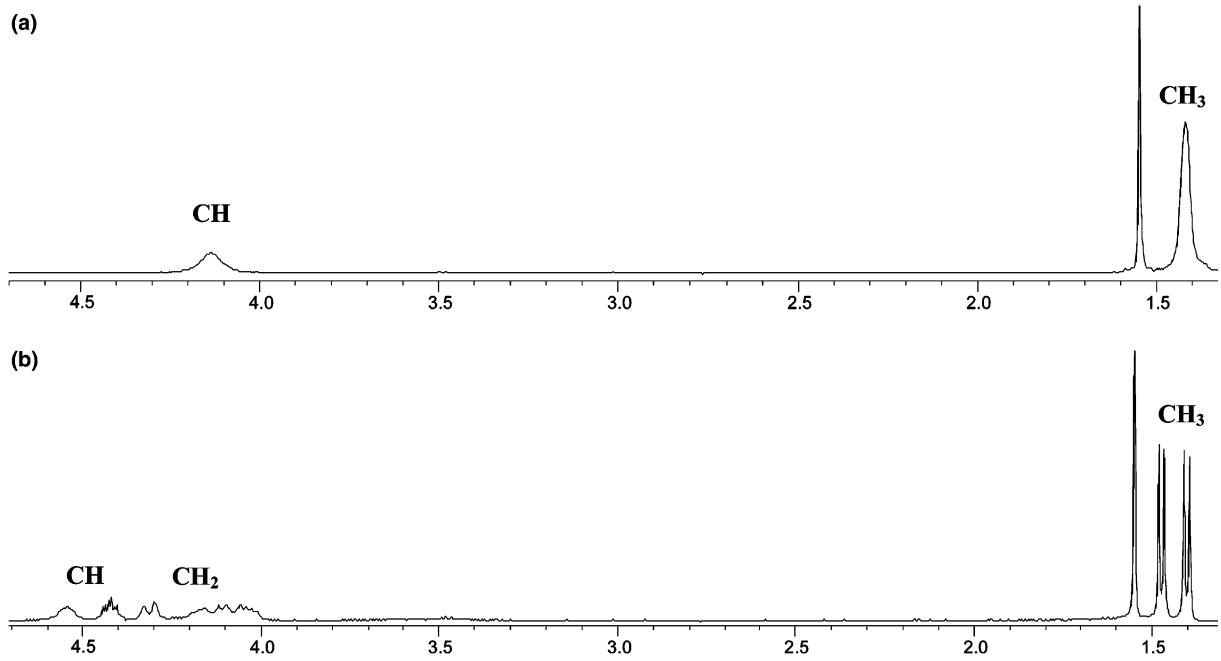

Fig. 5. ^{1}H NMR spectra in $CDCl_3$, at room temperature of: (a) [Pd(CH_3)(Cl)(bbpy)] (**4c**); (b) [Pd(CH_3)(Cl)(pbpy)] (**5c**): region of signals of protons of the bridge.

trans isomers. For the complexes with pbpy ligand, the rate of the equilibrium between the two atropisomers is slow on the NMR timescale.

2.2. CO/styrene copolymerization reaction

The monocationic complexes **1a**–**5a** and **1b**–**5b** have been tested as precatalysts in the CO/styrene copolymerization reaction, at $T = 30$ °C, under 1 atm of CO, in the presence of 1,4-benzoquinone as oxidant.

When dichloromethane is used as reaction medium, the productivities of all the complexes are modest and do not exceed the value of 650 g CP/g Pd (162 g CP/g Pd h; CP = copolymer; Fig. 6), obtained with complex **2b** (N–N = 3-*s*Bu-phen, X = OTf). The effect of the nature of the N–N ligand evidences that phen- and bpy-containing catalysts show very similar activities, while the productivities of complexes **4a**, **4b**, **5a** and **5b** are lower than that of simple bpy, in particular for the triflate derivatives. As recently observed for the bischelated complexes [Pd(3-R-phen)$_2$][PF_6]$_2$ [5c], an increase of productivity is found on going from phen to 3-*s*Bu-phen even for the monochelated compounds (Fig. 6(a)). Another analogy between the bischelated and monochelated complexes is related to the stability of the active species, which is lower with bipyridines than with phenanthrolines [5a]. These effects are not dependent on the counterion of the complex. The nature of the N–N ligand influences the molecular weight values in the case of the hexafluorophosphate derivatives, while almost no variation is observed when the triflate complexes are used (Fig. 7).

A remarkable effect of the anion on the productivity is found, being the triflate catalysts more active than the hexafluorophosphate derivatives (Fig. 6). This trend is the opposite of what generally reported in the literature for this reaction [13], and of what we found with the monocationic complexes [Pd(η^1,η^2-C_8H_{12}OMe)(bpy)][Y] (Y = BArF, SbF_6^-, PF_6^-, BF_4^-, OTf, BPh_4^-), where the highest activity was related to the complex with the least coordinating anion [11]. As far as the effect of the anion on the M_w values is concerned, the polyketones synthesized with phen or 3-*s*Bu-phen catalysts have similar M_w values regardless if the anion is PF_6^- or OTf (Fig. 7(a)), whereas when the ligands with bipyridine skeleton are used, the copolymers synthesized with the hexafluorophosphate derivatives have longer chains than those prepared with the triflate-catalysts (Fig. 7(b)).

A remarkable increase in the productivity is observed for all the catalysts tested when the polymerizations are carried out in trifluoroethanol, regardless of the nature of the N–N ligand and of the anion (Fig. 6). While for the catalysts containing phenanthrolines the increase in the productivity is from 1.5 to 3 times, in the case of the active species with bipyridines the differences of productivity in the two solvents are more pronounced and an enhancement of productivity of 5 times is generally found in TFE. The highest value of productivity per hour reached is of 363 g CP/g Pd h, obtained with precatalyst **5b**. This increase in the productivity is associated to an increase in the molecular weight values, even though it is not of the same entity. Within the range of time investigated no catalyst decomposition is observed

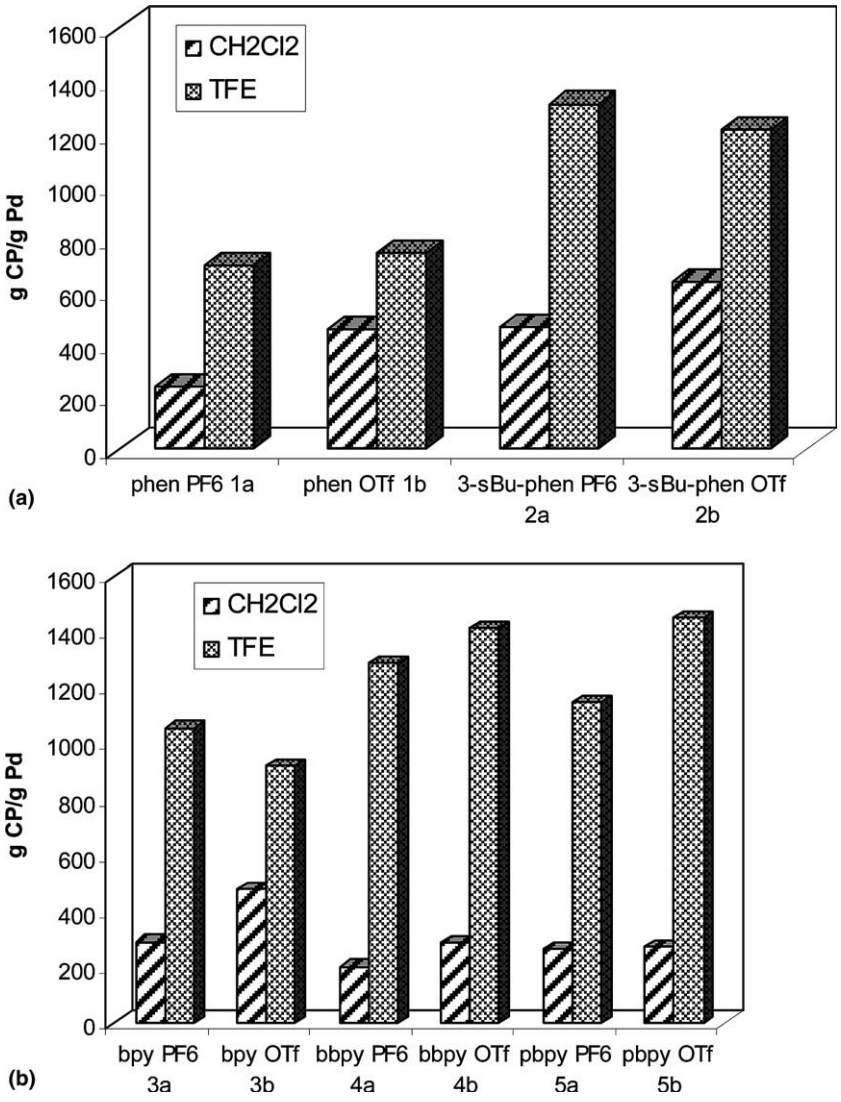

Fig. 6. CO/styrene copolymerization: effect of catalyst precursor on the productivity. Catalyst precursors: $[Pd(CH_3)(NCCH_3)(N–N)][X]$ (**1a**–**5a**, **1b**–**5b**). Reaction conditions: $n_{Pd} = 1.27 \times 10^{-5}$ mol; [BQ]/[Pd] = 40; $P_{CO} = 1$ atm; $T = 30$ °C; styrene $V = 10$ mL; [styrene]/[Pd] = 6800; solvent $V = 20$ mL; $t = 4$ h. (a) Catalysts with phen skeleton; (b) catalysts with bpy skeleton.

in TFE. Therefore, the positive effect of the fluorinated alcohol is due to the remarkable increase of stability of the active species and this is particularly evident in the catalysts with the bipyridine ligands that are the least stable in CH_2Cl_2. The enhancement of the length of the polymeric chains indicates that the fluorinated alcohol has also a positive effect on the ratio between the propagation and termination rate. However, on the basis of our results, it is not possible to discriminate if this effect consists in an increase of the insertion rate or in a decrease of the termination rate or in both of them.

The analysis of the effect of the N–N ligand on the productivity in trifluoroethanol evidences that the bpy catalyst is more active than the phen catalyst, regardless to the anion present, thus confirming that, once the problem of stability is solved, the bipyridine shows a higher specific activity than that of phen. As expected, the catalyst with the 3-alkyl-substituted phen is more active than that with the simple phen [5c]. On the opposite of what observed in dichloromethane, in trifluoroethanol the complexes with the atropisomeric ligands, **4a**, **4b**, **5a** and **5b,** are more active than the simple bpy (Fig. 6(b)). As observed in CH_2Cl_2, even in TFE the effect of the N–N ligand on the M_w values is more pronounced for the hexafluorophosphate catalysts than for the triflate derivatives (Fig. 7).

In TFE the effect of the anion on the productivity is less clear than in CH_2Cl_2 and it cannot be generalized for all the ligands tested. For instance, the hexafluorophosphate derivative **3a** is more active than the corresponding triflate complex **3b**, while in other cases the triflate species show a slightly higher activity than the

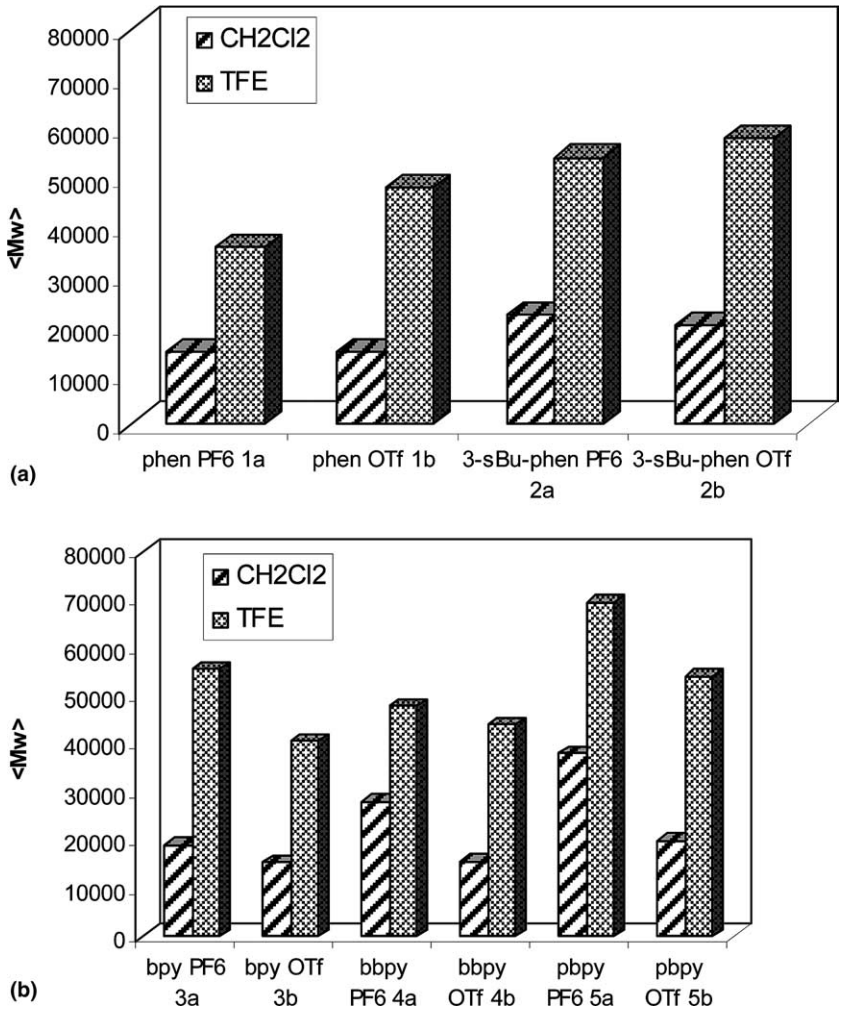

Fig. 7. CO/styrene copolymerization: effect of catalyst precursor on molecular weight. Catalyst precursors: $[Pd(CH_3)(NCCH_3)(N–N)][X]$ (**1a**–**5a**, **1b**–**5b**). Reaction conditions: see Fig. 6. (a) Catalysts with phen skeleton; (b) catalysts with bpy skeleton.

PF_6^- complexes (Fig. 6). The influence of the anion on the M_w values is analogous to what observed in CH_2Cl_2 (Fig. 7).

The effect of reaction time on productivity and molecular weight was evaluated with complex **1a** in both solvents (Fig. 8, Table 4). When the copolymerization is carried out in dichloromethane a slight increase of productivity is found during the first 8 h of reaction, followed by catalyst deactivation. A completely different catalytic behavior is shown in trifluoroethanol, where the productivity increases almost steadily with time and the value of 3.21 kg CP/g Pd is reached in 24 h. The comparison of the trend of productivity with time in the two solvents is analogous to that we reported when the catalytic behavior in TFE was compared with that in methanol [14], thus confirming the positive effect associated to the use of the fluorinated alcohol, even when monochelated complexes are the precatalysts.

The molecular weight values of the synthesized polyketones do not vary with time (Table 4), thus indicating that the chain transfer reaction is very efficient in both solvents. This result is in contrast with the linear enhancement of the length of the polymeric chains recently found by us, when the polymerizations are always carried out in TFE, but with the bischelated complexes $[Pd(3\text{-R-phen})_2][PF_6]_2$ and at a CO pressure of 40 atm [5c]. This analysis suggests that the coordination of both CO and the second molecule of N–N ligand favorably competes with the β-hydrogen elimination during the growing of the chain, retarding the chain transfer process.

Selected copolymerization experiments were carried out in both solvents with precatalyst **1a** in the absence of the oxidant (Table 5). In trifluoroethanol, for short reaction times the productivity is unaffected by the oxidant; on the other hand for longer reaction times (24 h) the benzoquinone effect is rather pronounced, being the productivity with no benzoquinone, at 24 h, 5 times lower than the value obtained when benzoquinone is present. This result is clearly related to the role played by the oxidant in the alcoholic medium. In agreement with the literature [14,15], the benzoquinone transforms the Pd–H

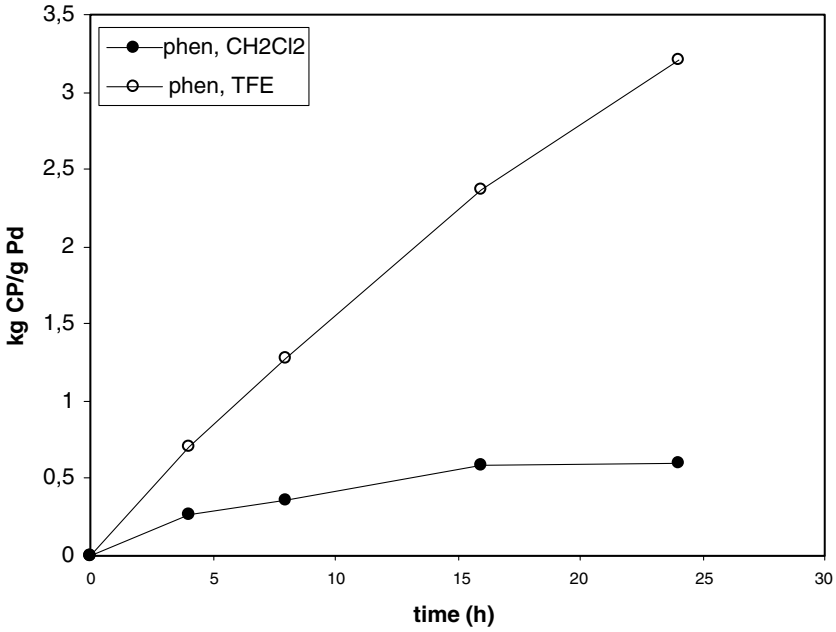

Fig. 8. CO/styrene copolymerization: effect of reaction time on productivity. Catalyst precursor: **1a**. Reaction conditions: see Fig. 6.

Table 4
CO/styrene copolymerization: effect of reaction time on molecular weight values in the two solvents

Time (h)	CH_2Cl_2		TFE	
	$\langle M_w \rangle$	$\langle M_w \rangle / \langle M_n \rangle$	$\langle M_w \rangle$	$\langle M_w \rangle / \langle M_n \rangle$
4	10,000	1.9	36,000	2.1
8	11,500	2.0	33,000	2.5
16	14,500	2.3	35,000	2.6
24	13,000	2.1	33,000	2.8

Catalyst precursor: $[Pd(CH_3)(CH_3CN)(phen)][PF_6]$ (**1a**).
Reaction conditions: see Fig. 6.

intermediate into the corresponding alkoxy derivative, on which a new polymeric chain can start to grow. When no benzoquinone is present, the new polymer initiates to grow through the insertion of styrene in the Pd–H intermediate (Scheme 3) [5c]. Therefore, the data obtained after 24 h of reaction reflect the different rate of these two pathways, confirming that the oxidation reaction of the Pd–H species, operated by benzoquinone, is much faster than the insertion of the olefin into the Pd–H bond.

Table 5
CO/styrene copolymerization: effect of benzoquinone in the two solvents. Catalyst precursor: $[Pd(CH_3)(CH_3CN)(phen)][PF_6]$ (**1a**)

Time (h)	[BQ]/[Pd] = 40 (kg CP/g Pd)	[BQ]/[Pd] = 0 (kg CP/g Pd)
Solvent = TFE		
4	0.31	0.45
24	3.21	0.68
Solvent = CH_2Cl_2		
4	0.26	0.20
24	0.60	0.30

Reaction conditions: see Fig. 6.

Surprisingly, the oxidant affects the productivity even when the copolymerization is carried out in dichloromethane (Table 5). In fact, the productivity is halved when no benzoquinone is added, together with fast decomposition of the catalyst. The origin of this effect appears to be less evident than in alcohol and it might be related to the presence of traces of water, which, in the presence of benzoquinone, can play the role of the alcohol; whereas without benzoquinone, in dichloromethane, the Pd–H species is not stable enough to allow the insertion of the olefin and to start a new catalytic cycle. It easily decomposes to palladium metal.

All the synthesized polyketones are mainly syndiotactic with the usual triads distribution in the corresponding ^{13}C NMR spectra.

2.3. Polyethylene synthesis

The study of the copolymerization reactions in trifluoroethanol evidences that the main role of the fluorinated alcohol consists in increasing the stability of the

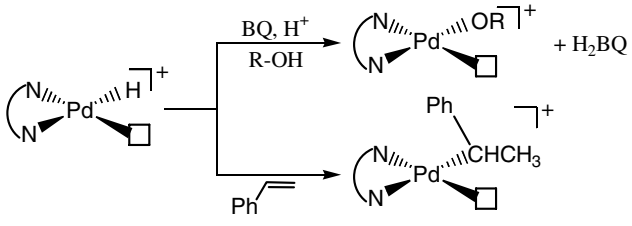

Scheme 3. The two pathways involving the Pd–H intermediate.

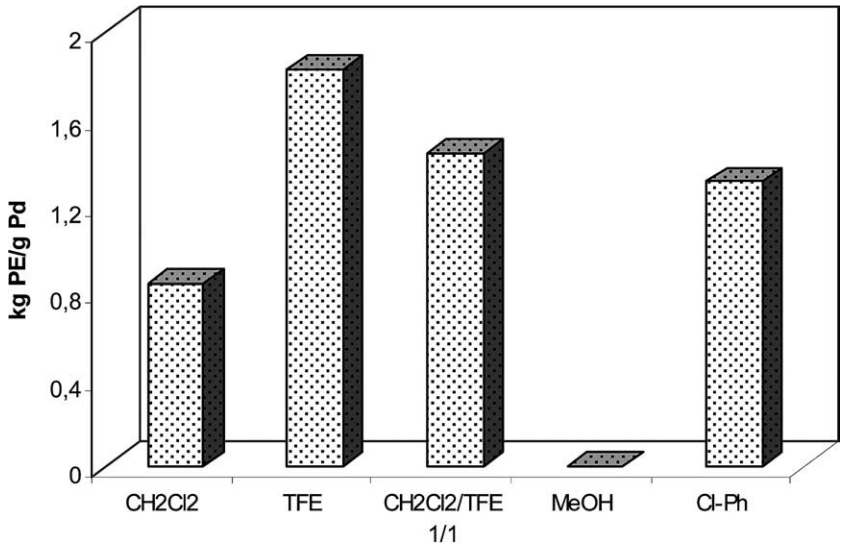

Fig. 9. Polyethylene synthesis: effect of solvent. Catalyst Precursor: $[Pd(CH_3)(NCCH_3)(iso\text{-}DAB)][PF_6]$ **6a**. Reaction conditions: $n_{Pd} = 1 \times 10^{-5}$ mol; $P_{C_2H_4} = 1$ atm; $T = 25$ °C; $t = 6$ h; solvent $V = 20$ mL.

Pd–H intermediate. To evaluate if this effect can be extended to other reactions involving the palladium-hydride species, we investigated the effect of the solvent in the polyethylene synthesis promoted by the precatalyst **6a** $[Pd(CH_3)(NCCH_3)(iso\text{-}DAB)][PF_6]$, differing from that reported by Brookhart in the labile ligand, which is acetonitrile instead of diethyl ether, and in the anion, which is hexafluorophosphate instead of BArF [3]. The homopolymerization reactions were carried out at $T = 25$ °C, under 1 atm of ethylene, with no addition of any initiator.

The catalytic tests, run for 6 h, evidence that the productivity of the system in trifluoroethanol is twice with respect to the value obtained in dichloromethane and that an intermediate value is found when the reaction is carried out in a 1:1 mixture of the two solvents (Fig. 9). The data of productivity in TFE is also higher with respect to the value reached in chlorobenzene (Cl–Ph). Finally, no reaction proceeds in methanol, where the catalyst decomposition takes place immediately. The difference of productivity between TFE and CH_2Cl_2 is kept even on prolonging the reaction time (Table 6).

The analysis of the molecular weight values shows a bimodal distribution for polyethylene synthesized in CH_2Cl_2, while monomodal curves are obtained for the polymers obtained in trifluorethanol and in chlorobenzene. The highest value of molecular weight was found for the polyethylene prepared in TFE, thus confirming the positive effect of this solvent in retarding the chain transfer process, even in the homopolymerization reaction (Table 7).

The comparison of ^{13}C NMR spectra of polyethylenes synthesized in dichloromethane and in trifluoroethanol indicates that in both cases the polymer has a highly branched microstructure. Therefore, no effect of the solvent on the chain walking with respect to the chain growing is observed.

Table 6
Polyethylene synthesis: effect of reaction time in the two solvents

Time (h)	kg PE/g Pd
Solvent = TFE	
4	1.37
24	2.30
Solvent = CH_2Cl_2	
4	0.84
24	0.92

Catalyst precursor: $[Pd(CH_3)(CH_3CN)(iso\text{-}DAB)][PF_6]$ (**6a**).
Reaction conditions: see Fig. 9.

Table 7
Polyethylene synthesis: effect of solvent on molecular weight

Solvent	M_w	M_w/M_n
CH_2Cl_2	172,000	1.18
	54,000	1.17
Cl–Ph	73,000	1.62
TFE	284,000	1.58

Catalyst precursor: $[Pd(CH_3)(CH_3CN)(iso\text{-}DAB)][PF_6]$ (**6a**).
Reaction conditions: see Fig. 9.

3. Conclusion

In conclusion, the positive effect of 2,2,2-trifluoroethanol as solvent has clearly been evidenced in the CO/styrene copolymerization catalyzed by different monochelated, organometallic palladium complexes leading to the synthesis of syndiotactic polyketones. An increase in the productivity up to 5 times is found

respected to the catalysis carried out in dichloromethane under the same conditions, associated to an increase of the molecular weight values of the polymers obtained. Studies of the effect of the reaction time showed the capability of TFE to increase remarkably the catalyst lifetime, since productivities still increase after 24 h, unlike what is observed for dichloromethane. The study of the effect of the solvent in the synthesis of the CO/vinyl arenes polyketones with an isotactic microstructure is under current investigation.

The positive role played by the fluorinated alcohol is clearly evidenced even in the homopolymerization of ethylene and this data represents the first time that polyethylene synthesis is performed in an alcoholic medium. Further investigations are also in progress in this field.

4. Experimental

4.1. General

The nitrogen-donor ligands (Aldrich) together with the analytical grade solvents (Carlo Erba) were used without further purification for synthetic and spectroscopic purposes. The 3-*s*Bu-phen was synthesized following the procedure reported in the literature [16]. The atropisomeric ligands, bbpy and pbpy, were prepared following the published procedure [8]. The dichloromethane used for both the synthesis of complexes and the catalytic reactions was purified through distillation over $CaCl_2$ and stored under inert atmosphere. $[Pd(CH_3COO)_2]$ was a loan from Engelhard Italiana. Carbon monoxide (CP grade, 99.9%) and ethylene (CP grade, 99.9%) were supplied by SIAD.

^1H and ^{13}C NMR spectra were recorded at 400 and 100.5 MHz, respectively, on a JEOL EX 400 spectrometer; the resonances were referenced to the solvent peak versus TMS ($CDCl_3$ at 7.26 δ for ^1H and 77.0 δ for ^{13}C; CD_2Cl_2 at 5.33 δ for ^1H and 53.8 δ for ^{13}C). Two-dimensional correlation spectra (COSY) were obtained with the automatic program of the instrument. The NOE experiments were run with ^1H pulse of 90° of 12.3 μs. ^{13}C NMR spectra of polyketones were recorded in 1,1,1,3,3,3-hexafluoro-2-propanol (HFIP) with a small amount of $CDCl_3$ for locking purposes. ^{13}C NMR spectra of polyethylenes were recorded in toluene-d_8. Elemental analyses (C, H, N), performed at Dipartimento di Scienze Chimiche (Università di Trieste), were in perfect agreement with the proposed stoichiometry (Table 8).

4.2. Synthesis of complexes

All manipulations were carried out in argon atmosphere by using Schlenk techniques and at room temperature, unless otherwise stated.

$[Pd(CH_3COO)_2]$, used as starting material, was transformed in *trans*-$[Pd(Cl)_2(PhCN)_2]$ following the procedure reported in the literature [6c]. $[Pd(Cl)_2(COD)]$ was obtained from *trans*-$[Pd(Cl)_2(PhCN)_2]$ [17]. The synthesis of $[Pd(CH_3)(Cl)(N–N)]$ (**1c**–**6c**) from $[Pd(Cl)_2(COD)]$ was made following the literature method [6a]. The monocationic complexes **1a**–**6a** and **1b**–**5b** were obtained according to the methods reported below:

*Synthesis of complexes [Pd(CH$_3$)(CH$_3$CN)(N–N)][X] (**1a**–**6a**, **1b**–**5b**).* The compounds $[Pd(CH_3)(CH_3CN)(N–N)][X]$, **1a**–**6a**, **1b**–**5b**, were synthesized mainly following the method reported in the literature [6c].

*Synthesis of complexes [Pd(CH$_3$)(CH$_3$CN)(N–N)][X] (**1a**–**5a**, **1b**–**5b**).* A solution of AgX (0.46 mmol in 8 mL of anhydrous acetonitrile) was added to a suspension of 0.40 mmol of $[Pd(CH_3)(Cl)(N–N)]$ in 10 mL of dichloromethane. After 30′ the formed AgCl was filtrated and the obtained solution was concentrated under vacuum, yielding a pale yellow solid upon addition of diethyl

Table 8
Elemental analyses of complexes **1a**–**6a** and **1b**–**5b**[a]

Compound	C (%)	H (%)	N (%)
$[Pd(CH_3)(NCCH_3)(phen)][PF_6]$ (**1a**)	37.3 (36.9)	2.69 (2.89)	8.40 (8.62)
$[Pd(CH_3)(NCCH_3)(phen)][OTf]$ (**1b**)	38.6 (39.1)	2.72 (2.87)	8.37 (8.54)
$[Pd(CH_3)(NCCH_3)(3\text{-}s\text{Bu-phen})][PF_6]$ (**2a**)	41.8 (42.0)	4.15 (4.08)	7.55 (7.73)
$[Pd(CH_3)(NCCH_3)(3\text{-}s\text{Bu-phen})][PF_6]$ (**2b**)	43.0 (43.8)	3.83 (4.05)	7.27 (7.67)
$[Pd(CH_3)(NCCH_3)(bpy)][PF_6]$ (**3a**)	33.2 (33.7)	2.82 (3.04)	8.82 (9.06)
$[Pd(CH_3)(NCCH_3)(bpy)][OTf]$ (**3b**)	35.2 (35.9)	3.14 (3.02)	8.22 (8.94)
$[Pd(CH_3)(NCCH_3)(bbpy)][PF_6]$ (**4a**)	36.5 (37.1)	4.10 (3.67)	7.42 (7.64)
$[Pd(CH_3)(NCCH_3)(bbpy)][OTf]$ (**4b**)	38.6 (39.0)	3.70 (3.64)	7.06 (7.59)
$[Pd(CH_3)(NCCH_3)(pbpy)][PF_6]$ (**5a**)	36.0 (35.9)	3.57 (3.39)	7.87 (7.84)
$[Pd(CH_3)(NCCH_3)(pbpy)][OTf]$ (**5b**)	37.1 (37.8)	3.43 (3.36)	7.43 (7.78)
$[Pd(CH_3)(NCCH_3)(iso\text{-}DAB)][PF_6]$ (**6a**)	51.7 (52.3)	6.64 (6.51)	5.77 (5.90)

[a] Calculated values are reported in parenthesis.

ether. The solid was filtered, washed with diethyl ether and dried under vacuum. Average yield: 75%.

*Synthesis of complex [Pd(CH$_3$)(CH$_3$CN)(iso-DAB)][PF$_6$] (**6a**).* A solution of $NaPF_6$ (0.46 mmol in 8 mL of anhydrous acetonitrile) was added at the suspension of [Pd(CH$_3$)(Cl)(iso-DAB)] in dichloromethane (0.40 mmol of **6c** in 10 mL of CH_2Cl_2) and the reaction was completed after 1 h. NaCl was removed by filtration, the solution was concentrated under vacuum and the addition of diethyl ether permitted to obtain a yellow solid that was filtered, washed with diethyl ether and dried under vacuum. Yield: 90%.

4.2.1. X-ray crystallography

Diffraction data for the structures reported were carried out on a Nonius DIP-1030H system with Mo Kα radiation (λ = 0.71073 Å, 30 frames for each experiment, exposure time of 15–20 min, rotation angle of 6° about φ, the detector at 80 (**4c′**) and 90 mm (**4a**, **6a**) from the crystal). Cell refinement, indexing and scaling of the data sets were carried out using programs Mosflm [18] and Scala [18]. All the structures were solved by Patterson and Fourier analyses [19] and refined by the full-matrix least-squares method based on F^2 with all observed reflections [19]. Two chloroform molecules were detected in the ΔF map of **4c′**. Due to the low number of reflections with $I > 2\sigma(I)$ the carbon atoms of pyridine rings of compound **4a** were treated isotropically. Crystal data and details of structure refinements are reported in Table 9. All the calculations were performed using the WinGX System, Ver 1.64.05 [20].

4.2.2. CO/styrene copolymerization

The copolymerization reactions were carried out in a glass reactor (75 mL), equipped with magnetic stirrer and temperature controller. The precatalyst, the 1,4-benzoquinone (when required), the aromatic olefin and the solvent were placed in the reactor; CO was bubbled for 10 min, then a 4 L balloon filled in with CO was connected to the reactor and the system was heated at 30 °C. After cooling and releasing the residual gas, the reaction mixture was poured into methanol (100 mL). The precipitated copolymer was separated by filtration, washed with methanol and dried under vacuum.

Recrystallization of CO/styrene polyketones. The CO/styrene polyketones were washed twice: first 1.00 g was suspended in 50 mL of ethyl acetate for 4 h, then filtered, dried under vacuum. Afterwards 1.00 g was suspended in 25 mL of diethyl ether for 2 h, filtered and dried under vacuum.

Table 9
Crystallographic data and details of structure refinements for compounds **4c′**, **4a** and **6a**

	4c′·$CHCl_3$	**4a**	**6a**
Formula	$C_{15}H_{15}Cl_5N_2O_2Pd$	$C_{17}H_{20}F_6N_3O_2PPd$	$C_{31}H_{46}F_6N_3PPd$
M_w	538.94	549.73	712.08
Crystal system	Triclinic	Monoclinic	Triclinic
Space group	*P*1	*C*2	$P\bar{1}$
a (Å)	8.756(3)	24.692(5)	10.675(3)
b (Å)	10.006(4)	12.399(4)	11.691(3)
c (Å)	12.721(4)	15.270(4)	15.230(4)
α (°)	105.23(2)		83.74(2)
β (°)	93.78(2)	106.85(3)	74.33(2)
γ (°)	69.07(2)		71.52(2)
Volume (Å^3)	1004.0(6)	4474(2)	1735.1(8)
Z	2	8	2
D_c (g/cm^3)	1.783	1.632	1.363
μ(Mo Kα) (mm^{-1})	1.601	0.967	0.637
F(000)	532	2192	736
θ_{max} (°)	28.99	26.37	27.10
Reflections collected	10839	23919	17212
Unique reflections	8056	9147	7128
R_{int}	0.0550	0.0585	0.0427
Observed $I > 2\sigma(I)$	6510	2796	5883
Parameters	451	441	392
Goodness-of-fit (F^2)	1.048	1.076	1.023
R_1 [$I > 2\sigma(I)$][a]	0.0449	0.0795	0.0497
wR_2 [a]	0.1189	0.1850	0.1342
Flack parameter	−0.02(4)	−0.04(10)	–
Δρ (e/Å^3)	0.501, −0.752	0.376, −0.376	0.670, −0.848

[a] $R_1 = \sum ||F| - |F|| / \sum |F|$, $wR_2 = \left[\sum w(F_o^2 - F_c^2)^2 / \sum w(F_o^2)^2\right]^{1/2}$.

4.2.3. Ethylene homopolymerization

The homopolymerization reactions were carried out in a glass reactor (75 mL), analogous to that used for CO/styrene copolymerizations. The precursor and the solvent were placed in the reactor. The air was removed making three vacuum/Ar cycles and after having made vacuum for the last time, two 4 L balloons filled in with ethylene were connected to the reactor. The reaction was heated at 25 °C. At the end of the reaction, the mixture was cooled, the residual gas was removed and the reaction mixture was added to methanol (100 mL), obtaining the precipitation of the polymer as a glue. The polymer was dissolved in petroleum ether 40–60 °C (100 mL), from which is obtained an oil by complete evaporation of the solvent.

Purification of polyethylene. Polyethylene was recrystallized: the polymer is dissolved in chloroform (100 mg in 50 mL of solvent), filtered over celite® and precipitated with ethanol. The solvent is completely removed under vacuum yielding the polymer as an oil.

4.2.4. Molecular weight measurements of CO/styrene polyketones

The molecular weights (M_w) of CO/styrene copolymers and the molecular weight distributions (M_w/M_n) were determined by gel permeation chromatography versus polystyrene standards. The analyses were recorded on a Knauer HPLC (K-501 Pump, K-2501 UV-detector) with a PLgel 5 μm 10^4 Å GPC column and chloroform as solvent (flow rate 0.6 mL/min). Samples were prepared as follows: 2 mg of the copolymer was solubilized with 120 μL of 1,1,1,3,3,3-hexafluoro-2-propanol (HFIP) and chloroform was added up to 10 mL. The statistical calculations were performed using the Bruker Chromstar software program.

4.2.5. Molecular weight measurements of polyethylene

Molecular weight determination is performed by Alliance GPCV 2000 Series System from Waters Society (Milford, USA). This system includes a differential RI detector and a multicapillary viscosimetry detector. The data are then processed by Millennium® GPCV software to characterize the molecular weight distribution of the polymers. The following experimental conditions were used: columns: four Styragel Waters (HT6E: PM = 1×10^7–5000; two HT4: PM = 600,000–5000, HT3: PM = 30,000–500), solvent, mobile phase: 1,2,4-trichlorobenzene (TCB); temperature: 145 °C; flow rate: 1 ml/min; injection volume: 220.5 μL; calibration: relative and universal are obtained by 16 polystyrene standards at narrow MMD with molecular weight between 1,600,000 and 2000 g/mol; antioxidant protection: 0.5–1% Irganox 3052; sample solubilization: oven to 150 °C for more than 3 h.

5. Supplementary material

Crystallographic data for the structures reported have been deposited with the Cambridge Crystallographic Data Centre, CCDC No. CCDC 255246–255248. Copies of this information may be obtained free of charge from The Director, CCDC, 12 Union Road, Cambridge CB2 1EZ, UK (fax: +44-1223-336033; e-mail: deposit@ccdc.cam.ac.uk or www: http://www.ccdc.cam.ac.uk).

Acknowledgments

This work was supported by Ministero dell'Istruzione, dell'Università e della Ricerca (MIUR-Rome; PRIN Nos. 2003033857 and 2003039774) and by the European Network "PALLADIUM" (5th Framework Program, Contract No. HPRN-CT-2002-00196). Engelhard Italiana is gratefully acknowledged for a generous loan of $[Pd(CH_3COO)_2]$.

References

[1] (1) G.W. Coates, P.D. Hustad, S. Reinartz, Angew. Chem., Int. Ed. 41 (2002) 2237;
(1) G.W. Coates, J. Tiang, Angew. Chem., Int. Ed. 39 (2000) 3626.
[2] (2) S.D. Ittel, L.K. Johnson, M. Brookhart, Chem. Rev. 100 (2000) 1169;
(2) V.C. Gibson, S.K. Spitzmesser, Chem. Rev. 103 (2003) 283.
[3] L.K. Johnson, C.M. Killian, M. Brookhart, J. Am. Chem. Soc. 117 (1995) 6414.
[4] (a) E. Drent, Eur. Pat. Appl. 229408, 1986 (Chem. Abstr. 108 (1988) 6617);
(b) M. Barsacchi, G. Consiglio, L. Medici, G. Petrucci, U.W. Suter, Angew. Chem., Int. Ed. Engl. 30 (1991) 989;
(c) M. Brookhart, F.C. Rix, J.M. De Simone, J.C. Barborak, J. Am. Chem. Soc. 114 (1992) 5894;
(d) M. Brookhart, M.I. Wagner, G.G.A. Balavoine, H.A. Haddou, J. Am. Chem. Soc. 116 (1994) 3641;
(e) B. Bartolini, C. Carfagna, A. Musco, Macromol. Rapid Commun. 16 (1995) 9;
(f) K. Nozaki, N. Sato, H. Takaya, J. Am. Chem. Soc. 117 (1995) 9911;
(g) M.T. Reetz, G. Aderlein, K. Angermund, J. Am. Chem. Soc. 122 (2000) 996;
(h) A. Bastero, A. Ruiz, C. Claver, S. Castillon, Eur. J. Inorg. Chem. (2001) 3009;
(i) G. Consiglio, B. Milani, Stereochemical aspects of cooligomerization and copolymerization, in: A. Sen (Ed.), Catalysis by Metal Complexes, Kluwer Academic Publishers, Dordrecht, 2003.
[5] (a) B. Milani, G. Corso, G. Mestroni, C. Carfagna, M. Formica, R. Seraglia, Organometallics 19 (2000) 3435;
(b) B. Milani, A. Scarel, G. Mestroni, S. Gladiali, R. Taras, C. Carfagna, L. Mosca, Organometallics 21 (2002) 1323;
(c) A. Scarel, B. Milani, E. Zangrando, M. Stener, S. Furlan, G. Fronzoni, G. Mestroni, S. Gladiali, C. Carfagna, L. Mosca, Organometallics 23 (2004) 5593.
[6] (a) R.E. Rülke, J.M. Ernesting, A.L. Spek, C.J. Elsevier, P.W.N.M. van Leeuwen, K. Vrieze, Inorg. Chem. 32 (1993) 5769;

(b) J.H. Goren, J.G.P. Delis, P.W.N.M. van Leeuwen, K. Vrieze, Organometallics 16 (1997) 68;
(c) B. Milani, A. Marson, E. Zangrando, G. Mestroni, J.M. Ernsting, C.J. Elsevier, Inorg. Chim. Acta 327 (2002) 188.

[7] (a) A. Bastero, A. Ruiz, C. Claver, B. Milani, E. Zangrando, Organometallics 21 (2002) 5820;
(b) A. Bastero, C. Claver, A. Ruiz, S. Castillon, E. Daura, C. Bo, E. Zangrando, Chem. Eur. J. 10 (2004) 3747.

[8] B. Milani, E. Alessio, G. Mestroni, E. Zangrando, L. Randaccio, G. Consiglio, J. Chem. Soc., Dalton Trans. (1996) 1021.

[9] R.S. Cahn, C. Ingold, V. Prelog, Angew. Chem., Int. Ed. Engl. 5 (1966) 385.

[10] (a) D.J. Temple, L.K. Johnson, R.L. Huff, P.S. White, M. Brookhart, J. Am. Chem. Soc. 122 (2000) 6686;
(b) J. Feldman, S.J. McLain, A. Parthasarathy, W.J. Marshall, J.C. Calabrese, S.D. Arthur, Organometallics 16 (1997) 1514.

[11] A. Macchioni, G. Bellachioma, G. Cardaci, M. Travaglia, C. Zuccaccia, B. Milani, G. Corso, E. Zangrando, G. Mestroni, C. Carfagna, M. Formica, Organometallics 18 (1999) 3061.

[12] The detailed analysis of the interconversion of the different atropisomers is under investigation. J. Durand, E. Zangrando, C. Carfagna, B. Milani, manuscript in preparation.

[13] E. Drent, P.H.M. Budzelaar, Chem. Rev. 96 (1996) 663.

[14] B. Milani, A. Anzilutti, L. Vicentini, A. Sessanta o Santi, E. Zangrando, S. Geremia, G. Mestroni, Organometallics 16 (1997) 5064.

[15] E. Drent, J.A.M. van Broekhoven, M.J. Doyle, J. Organomet. Chem. 417 (1991) 235.

[16] S. Gladiali, G. Chelucci, M.S. Mudadu, M.A. Gastaut, R.P. Thummel, J. Org. Chem. 66 (2001) 400.

[17] L. Chatt, L.M. Vallarino, L.M. Venanzi, J. Chem. Soc. (1957) 3413.

[18] Collaborative Computational Project, Number 4. Acta Crystallogr. D 50 (1994) 760–763.

[19] G.M. Sheldrick, SHELX97: Programs for Crystal Structure Analysis (release 97-2), University of Göttingen, Göttingen, Germany, 1998.

[20] L.J. Farrugia, J. Appl. Crystallogr. 32 (1999) 837.